Egyptian Journal of Petroleum (2014) 23, 331–338

HOSTED BY

Egyptian Petroleum Research Institute

Egyptian Journal of Petroleum

www.elsevier.com/locate/egyjp
www.sciencedirect.com

FULL LENGTH ARTICLE

Physico-chemical characteristics of nano-organo bentonite prepared using different organo-modifiers

A.M. Motawie [a], M.M. Madany [b], A.Z. El-Dakrory [c], H.M. Osman [d], E.A. Ismail [a], M.M. Badr [a], D.A. El-Komy [a], D.E. Abulyazied [a,*]

[a] Petrochemical Department, Polymer Laboratory, Egyptian Petroleum Research Institute (EPRI), Nasr City, Cairo, Egypt
[b] Radiation Physics Department, National Center for Radiation Research and Technology, Nasr City, Cairo, Egypt
[c] Physical Department, Faculty of Girls, Ain Shams University, Cairo, Egypt
[d] Physical Department, Faculty of Science, Cairo University, Giza, Egypt

Received 3 September 2013; accepted 31 October 2013
Available online 11 November 2014

KEYWORDS

Nano-bentonite;
Hexadecyl trimethyl ammonium bromide;
3-Amino-propyltriethoxysilane;
Octadecylamine;
Dodecylamine

Abstract Different types of nano-organo bentonite (NOB) were prepared from the Egyptian Bentonite (EB). EB was characterized by energy dispersive X-ray EDX. It was purified from different impurities using a conventional method via the treatment with HCl and distilled water. The modification of the clay was carried out using different types of organo-modifiers namely; hexadecyl trimethyl ammonium bromide (HTAB), 3-aminopropyltriethoxysilane (Silane), octadecylamine (ODA), and dodecylamine (DDA). The cation exchange capacity (CEC) was measured for pristine bentonite after and before modification. The NB was characterized by FTIR, XRD, TEM, and TGA techniques. The obtained results indicated that variation of the interlayer space gallery was effected by the type of the penetrator used.

1. Introduction

Cationic nanoclays, as exemplified by smectites, contained a group of 2:1-layer minerals that included the hydrated aluminum silicates such as montmorillonite (MMT). In such minerals, the anionic charge of the alumina-silicate layer was neutralized by the intercalation of compensating exchangeable cations (e.g. Na^+, Ca^{2+} and/or Mg^{2+}) and their coordinated water molecules. MMT consisted of thin platelets of less than 1 nm thickness. Each aluminum octahedral layer was linked together by oxygen and was sandwiched between silicon tetrahedral layers. These layers were linked together by Van der Waals forces and were formed as stacks of plates. Each platelet had a large surface area and a high aspect ratio of over 200. A schematic of the MMT structure is shown in Fig. 1 [1–4].

In the modification of montmorillonite by ion exchange, the interlayer accessible compensating cations could be exchanged with a wide variety of hydrated inorganic cations or organic cations including those of amines or quaternary ammonium salts such as oxonium, sulfonium, phosphonium ions. In the meantime, more complex cationic species such as methylene blue and cationic dyestuffs had been used. The hydrophilicity of the modified mineral decreased and the basal spacing of the alkyl ammonium derivatives increased with increasing alkyl

* Corresponding author.
Peer review under responsibility of Egyptian Petroleum Research Institute.

http://dx.doi.org/10.1016/j.ejpe.2014.08.009

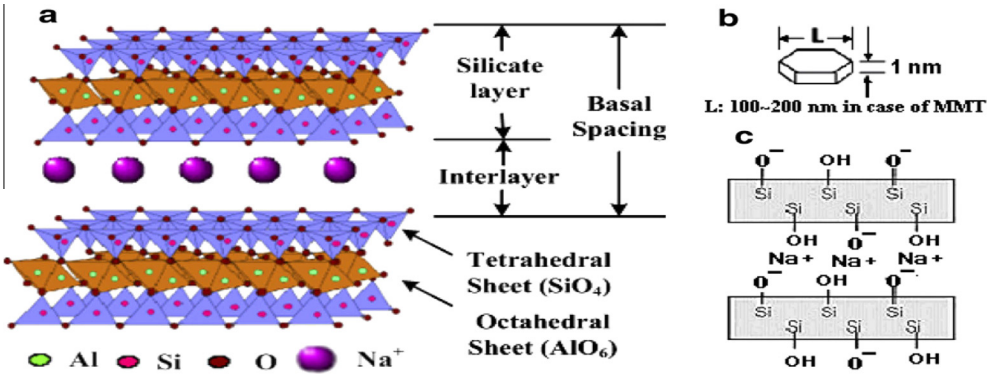

Figure 1 (a) Molecular structure of MMT containing exchangeable sodium ion (MMT-Na +), (b) high aspect ratio clay platelet, and (c) schematic representation of side view between layers. Adapted from Refs. [2–4].

chain length of the ammonium salts [5]. Commercial Organophilic montmorillonite used in the polymer nano-composites was usually prepared from the Na^+ MMT form by ion exchange with long chain (C16–C18) alkyl ammonium-based ions. In order to obtain good interfacial adhesion and mechanical properties, the hydrophilic clay needs to be modified prior to the introduction in most Organophilic polymer matrices [6].

Inorganic fillers were originally incorporated into polymers in order to produce cheaper materials. Soon it was discovered that the use of such fillers resulted in improving the polymer properties, e.g., stiffness, toughness, chemical resistance, barrier properties and thermal stability. The changes in the properties depended on several factors such as the size and shape of the filler particles and the interactions between the particles and the polymer matrix. The most abundant natural and inexpensive class of filler materials are the clays [7].

Polymer/clay mineral silicate nanocomposites had replaced conventional composites in a variety of applications due to their light mass coupled with enhanced properties. The four main properties considered are mechanical (automotive industry, etc.), barrier (packaging, film, bottle industry, etc.), fire retardancy (cable industry, etc.) and physical and optical (electronic industry, batteries) [8,9]. Some studies were carried out on clay minerals intercalated with alkyl ammonium ions [10–14]. These organo-clays were widely used in polyurethane coatings during processing. Polyurethane (PU)/organo-montmorillonite nanocomposites were prepared by in situ polymerization of toluene diisocyanate and 1,4-butanediol in the presence of different contents of organo-montmorillonite (9–18 mass%). Polymethylmethacrylate (PMMA)/Organophilic montmorillonite (OMMT) nanocomposites were synthesized by the in situ free radical bulk polymerization of methyl methacrylate [15].

The main objective of the present work was to synthesize different types of organo bentonite using different organo modifiers namely, hexadecyl trimethyl ammonium bromide (HTAB), 3-aminopropyl triethoxysilane (Silane), octadecylamine (ODA), and dodecyl amine (DDA). Various characteristics of the prepared organo-bentonites were studied using FTIR, XRD, TEM and TGA techniques.

2. Experimental

Hexadecyl trimethyl ammonium Bromide (HTAB) $CH_3(CH_2)_{15}N^+(CH_3)_3Br^-$, 3-aminopropyl triethoxysilane (Silane) $NH_2–CH_2–CH_2–CH_2–Si(OCH_2CH_3)_3$, octadecylamine (ODA) $CH_3(CH_2)_{17}NH_2$, dodecyl amine (DDA) $CH_3(CH_2)_{11}NH_2$, hydrochloric acid and sodium chloride, were provided by Aldrich Chemical Co., USA.

Table 1 The physical properties of bentonite.

Properties	Results
Yield M3/ton	17.4
Water loss MI	14.2
Moisture content%	10
Dry screen analysis passing Us 100 Mesh	99.5
Wet screen analysis passing Us 100 Mesh	98.5
Ph (5% con.)	9.0
Sand content %	0.2
Liquid limit %	400–500
Plastic limit %	30%
Plasticity index %	370–470
F.M.F (4% Con.) Sec	35

2.1. Purification process of the EB [16]

Egyptian Bentonite Clay (EB) was kindly provided by the Egyptian Bentonite Derivatives Company, from the western area of Al-Hamam, Alexandria, Egypt. Then, the 325 mesh sieve was only used. The physical properties of the EB are illustrated in Table 1 according to the data sheet received from the Fields Development Technology Center, the Egyptian Petroleum Research Institute, Nasr City, Cairo, Egypt.

EB was purified to remove impurities, i.e., carbonates, iron hydroxide and organic matter. A suspension in distilled water enabled us to obtain, a colloidal suspension after 12 h. The clay used was purified by sedimentation. It was treated with 0.05 M HCl in order to remove carbonates, followed by the treatment with oxygenated water in order to eliminate the organic matters.

2.2. Preparation of the activated bentonite Na-B [17,18]

The pure EB was saturated three times with sodium ions by stirring for 1 h in a 1 M sodium chloride solution. Then, the filtered solid was washed with distilled water to remove the excess salt. Na-B was dried at 110 °C, grounded and sieved

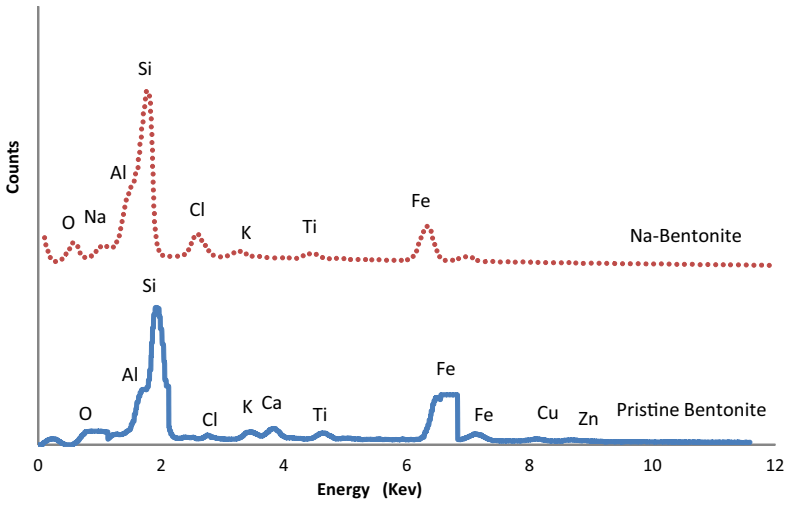

Figure 2 EDX spectra of raw and sodium exchanged bentonite.

into a 325 mesh in order to reduce agglomeration. The ball mill was not used since it increased the structural disorder and peeling off the layers from the particles, followed by the exfoliation of the particles [19]. The purification of the Na-bentonite was evaluated by the energy dispersive X-ray (EDX) process. The EDX is presented in Fig. 2. It indicated that, Cu, Zn, and Ca cations in pristine bentonite EB were exchanged with Na cation in the investigated Na-bentonite (Na-B).

2.3. Preparation of nano-bentonite NB

The nano-bentonites were synthesized by ion exchange reaction between Na-bentonite and different surfactants namely; hexadecyl trimethyl ammonium bromide (HTAB) [20,21], 3-aminopropyltriethoxysilane (Silane) [22], octadecylamine (ODA), and dodecylamine (DDA) [23]. The solution of the ammonium salt used was heated at 80 °C for a few minutes. The surfactants were protonated by adding HCl. Aqueous suspension 0.5 wt% of Na-B was also prepared and heated at 80 °C. The prepared alkyl ammonium salt solution was added drop-wise to the Na-bentonite suspension and maintained at 80 °C for 12 h under vigorous stirring. Then, the suspension was cooled to room temperature. The equation for calculating the intercalating agent needed for a cation-exchange reaction was [24]:

$$120/100 \times \text{grams of clay} \times 1.5 = (X/M_w \text{ of intercalating agent}) \times 1 \times 1000$$

where, X represents the amount of intercalating agent used, 120/100 represents the cationic exchange capacity (CEC) of 120 mEq/100 g of the clay, and 1.5 (> 1) is the alkyl amine/clay ratio and it indicated an excess amount of the intercalating agent used. The molar alkyl amine/HCl ratio was 1:1. The cation exchange capacity of the resulted clay was 120 mEq/100 g.

Finally, the treated clay particles were collected by centrifugation and subsequently washed with deionized water several times to remove the residual chloride or cations until no halides were detected in the filtrate by the Ag NO_3 test. The dispersion and washing were accomplished using a 50/50 ethanol/water mixture. The filter cake was then placed in a vacuum oven at 80 °C for 24 h. The dried cake was ground and screened with a 325-mesh sieve to obtain the inorganic-organophilic materials CTAB-B, ODA-B, DDA-B, and Silane-B.

2.4. Characterization techniques

Fourier-Transform Infrared Analysis (FTIR), operated in the transmission mode, in the wave number range of 4000–400 cm^{-1} was carried out by mixing with K Br powder on a Mattson 1000, series LC operating, Issue I (0791) spectrophotometer. The concentration of the samples in the K Br was held constant at 0.7% (w/w). Spectra were obtained using a resolution of 4 cm^{-1} and were averaged over 100 scans. The standard software (Omni ESP, version 5.1) was used for the data acquisition and analysis. X-ray diffraction pattern of different forms had been investigated using a modern PAN analytical diffractometer, Xpert PRO model. Nickel filtered cupper radiation (λ = 1.542 Å) technique was used. All the diffraction patterns were examined at room temperature and under constant operating conditions (40 kV and 40 mA). The scanning rate was 1 degree (2θ/min). The studied samples were grounded to a fine powder form and mounted in the appropriate aluminum folder. The Morphology was studied using the TEM-1230 model with an accelerating voltage of 100 kV (JEOL Co., Japan). The thermo-gravimetric analysis (TGA) was performed with a Shimadzu TGA-50H using 8–10 mg sample. The samples were heated at a rate of 10 °C/min in the range 50–790 °C in nitrogen atmosphere.

3. Results and discussion

3.1. FTIR analysis

The FTIR spectra of the unmodified Na-B and the nano-bentonite with the four different modifiers are shown in Fig. 3.

FTIR spectrum of Na-B indicated that, the OH bending band at 915 cm^{-1} was readily assigned to Al–OH. The strong band centered at 1029 cm^{-1} was the Si–O stretching vibration together with those at 524 and 463 cm^{-1} which indicated the Si–O–Al and Si-O–Si bending vibrations, respectively that were typical of the tetrahedral Si–O. Bands at 3426 and 1637 cm^{-1} were attributed to the OH stretching and bending vibrations of molecular water, respectively [25,26]. Band at 1475 cm^{-1} was assigned to the presence of carbonate [27].

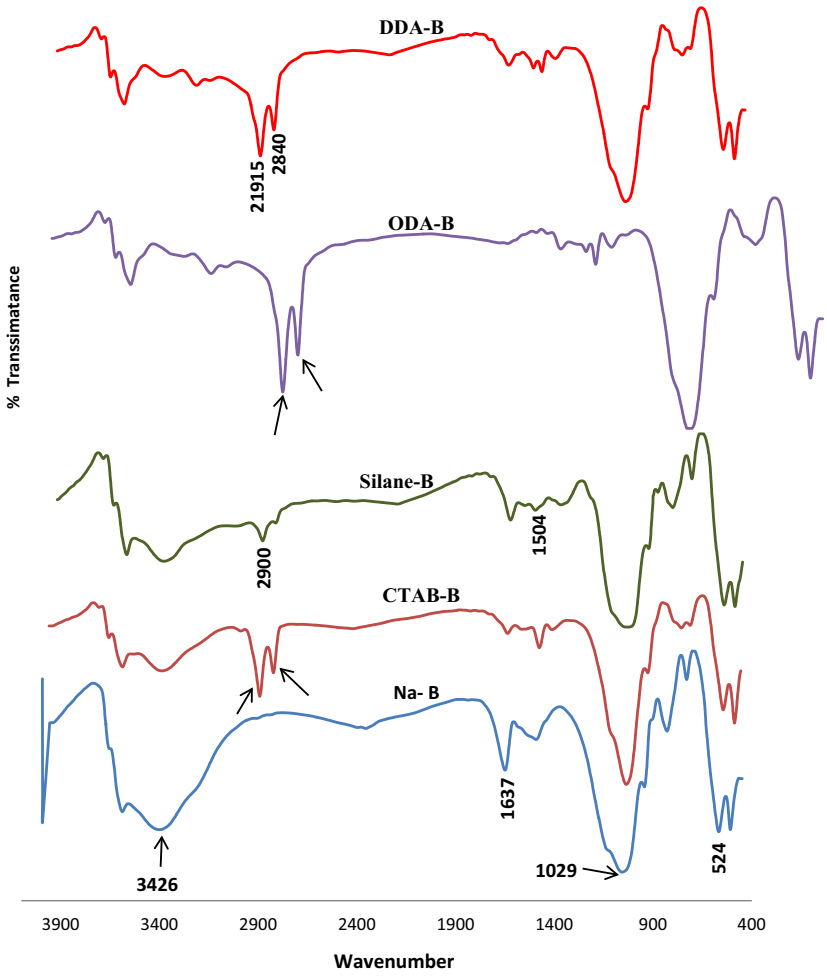

Figure 3 FTIR spectrum of unmodified Na-B and modified OB.

The spectra of NBs gave all the previous bands appeared in the FTIR spectrum of Na-B. These bands are related to the basic skeleton of the bentonite.

For the modified bentonites HTAB-B, ODA-B and DDA-B, peaks at 2915 and 2840 cm^{-1} were assigned to the stretching vibrations of $–CH_2$ and $–CH_3$, respectively indicating the presence of long alkyl chain in the bentonite [20,23]. Bands at 3426 and 1637 cm^{-1} were attributed to the OH molecular water disappeared. This indicated complete exchange of basal cations with the removal of water molecules [27].

The FTIR spectrum of the modified bentonite Silane-B displayed almost the same pattern as that of the unmodified bentonite, except for some new bands at 2935 cm^{-1} with a small hump at 2850 cm^{-1} that are due to the –CH asymmetric and symmetric stretching of the methylene groups (methylene groups of the amino silane) which confirmed the presence of the Silane surfactant on the surface. Also, new peak at 1504 cm^{-1} that corresponded to the $–CH_2$ bending vibrations further supported this conclusion. These peaks were confirmed by another published work [28].

3.2. X-ray diffraction

XRD patterns and values of the d-spacings d_{001} of the silicate-gallery for Na-B and the prepared samples of NBs are shown in Fig. 4.

It is clear from the pattern that, from 2θ = 2–10°, the Na-B has a single characteristic diffraction peak at (2θ) = 7.0° indicating that the d-spacing of the silicate layers was about 1.2 nm [29].

A shift of the d-spacing of the modified bentonites to lower diffraction angles when compared to the unmodified Na-B, is shown in Fig. 4. These results revealed that the layer galleries of the bentonites were expanded due to the modification of the different surfactants, which contained a long-chain alkyl group. The d-spacing of the nano-bentonites increased in the following order:

ODA-B > DDA-B > Silane-B ≃ HTAB-B.

The higher extent of the intercalation corresponded to the largest interlayer distance of 3.09 n at 2θ = 2.9° in ODA-B as compared with 1.26 nm for Na-B. This value of d-spacing indicated that ODA gave high separation for the clay layers. It was also shown from the pattern that ODA-B had another characteristic peak at 2θ = 5.7° corresponding to the basal spacing of 1.55 n. The changes of the interlayer spacing suggested the successful modification of Na-B, these results were also obtained by Zheng et al. [30] which will be confirmed by the TEM images.

For the two modifiers HTAB and DDA with different alkyl chain lengths, it was expected that HTAB-B gave higher interlayer distance (d) than DDA-B, because it had

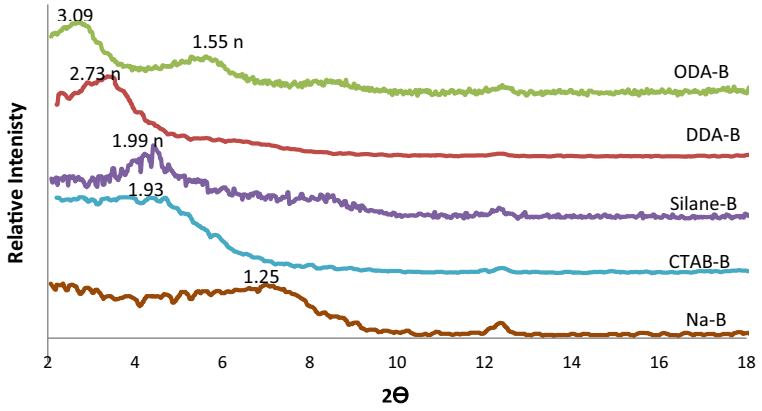

Figure 4 XRD pattern of pristine Na-B and different OBs.

a longer alkyl chain. However, it gave smaller d than DDA-B which was attributed to a decrease in the Bronsted acidity in HTAB. Where the decrease in the interlayer spacing with a decreasing Bronsted acidity of the exchange ion follows the order [31]:

$$\begin{aligned} CH_3(CH_2)_{15}NH_3^+ &> CH_3(CH_2)_{15}NH^+(CH_3)_2 \\ &> CH_3(CH_2)_{15}NH^+(CH_3)_2 \\ &> CH_3(CH_2)_{15}N(CH_3)_3^+. \end{aligned}$$

The data of the d-spacing shown in Fig. 4 illustrated that the d-spacing difference between the Na-B and Silane-B samples is about 0.73 nm. The increase in the basal spacing suggested that the poly-condensates could be formed in the interlaminate space. This is understandable because the silane preferentially replaced the sodium ions on the surface of the bentonite platelets with ammonium ions from the silane and these are grafted at the edge of the bentonite platelets due to the existence of a hydroxyl group at the edge of the bentonite platelets [32,33].

3.3. Transmission electron microscope (TEM)

Confirming XRD results, typical TEM images of the unmodified Na-B and the modified NBs at two different magnifications are shown in Figs. 5 and 6, respectively.

The photographs of the Na-B (Fig. 5a and b) indicated that there was no basal space between silicate layers, so individual silicate sheets could not be specified [34,35].

It was also shown from the photographs of the nano-bentonites (Fig. 6a–h) that the silicate layers were separated to some thin lamellas with different thicknesses relative to every modifier, where ODA-B samples (Fig. 6e and f) showed the best dispersion of bentonite followed by DDA-B samples (Fig. 6g and h). These data were in accordance with those of XRD, which showed that the ODA compound is the best modifier for bentonite then followed by DDA compound.

3.4. Thermal gravimetric analysis (TGA)

Thermal gravimetric analysis (TGA) was conducted under nitrogen atmosphere in order to investigate the thermal stability of NBs. TG curves of Na-B and NBs were collected for comparison as shown in Fig. 7. The thermo-gram of Na-B showed two thermal degradation transitions. The first transition at 100 °C, with 6.5% weight loss could be attributed to the evolution of desorbed water molecules. These water molecules were associated with the cations in the interlayer of the bentonite. These water molecules were loosely attached to crystals and evaporate at low temperatures.

The second transition of 9% weight loss at 526 °C could be assigned to the removal of water of crystallization. These water molecules trapped in the crystal lattice required a much higher temperature than the associated ones [36–38].

From the curves of the nano-bentonites, it is shown that the first weight loss in Na-B curve related to removal of water from the clay gallery, disappeared during the preparation step. This indicates complete removal of water and associated cations. The second thermal transition of the crystal water

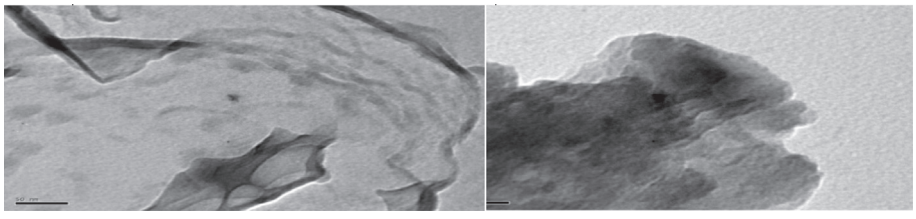

Figure 5 TEM images of Na-B (a) low magnification (b) high magnification.

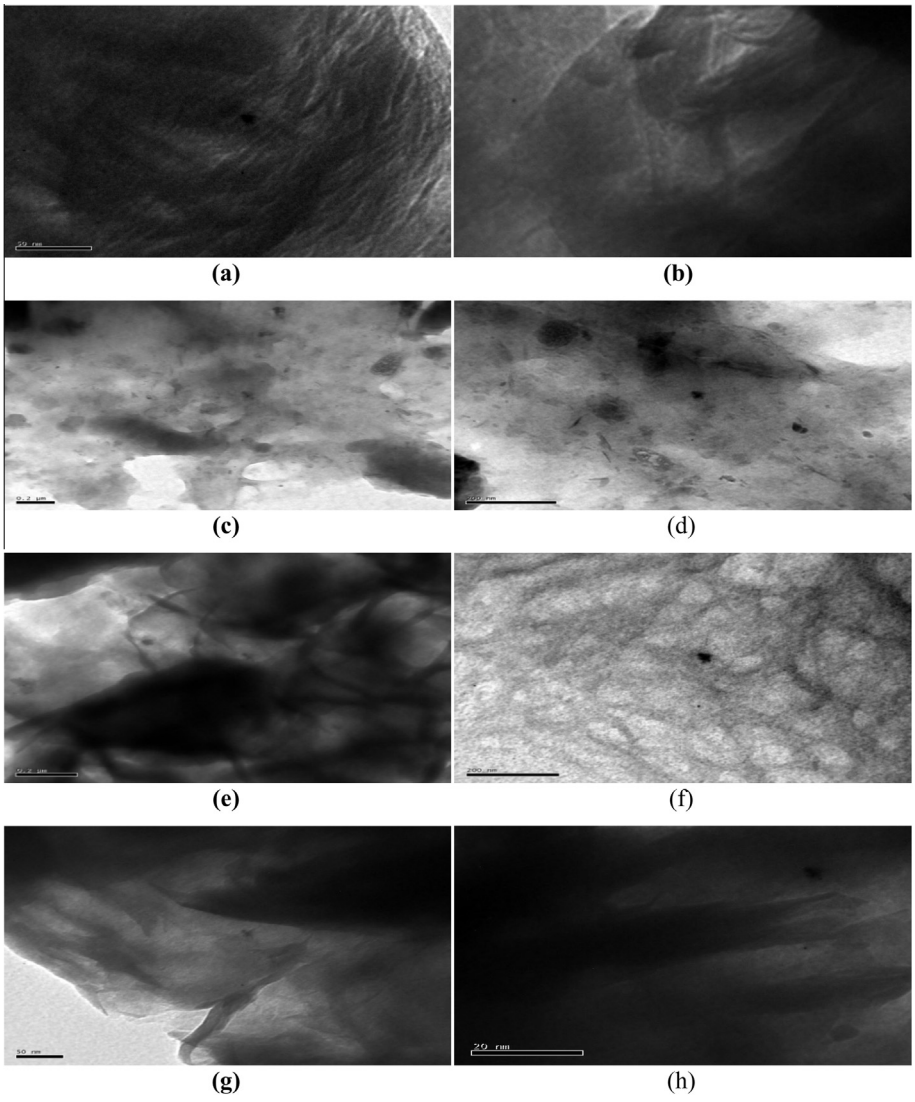

Figure 6 TEM images of OBs: (a, b) CTAB-B; (c, d) Silane-B; (e, f) ODA-B and (g, h) DDA-B at two different magnifications.

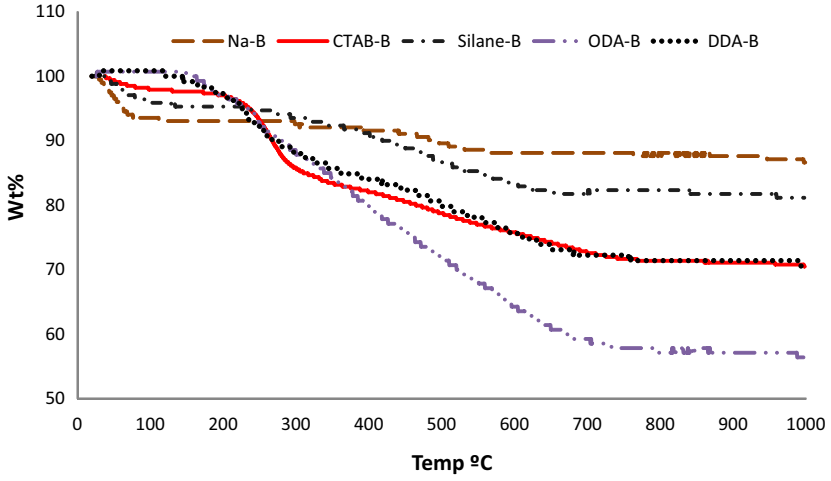

Figure 7 TGA curves of unmodified Na-B and OBs.

Table 2 The exchanged amounts of the modifiers in the bentonite gallery.

Sample symbol	CTAB-B	Silane-B	ODA-B	DDA-B
Exchanged organo-surfactant amount (mmol/100 g)	50	30	55	50
Main chain carbon number	17	3	18	12

removal collapsed with the thermal degradation of the organic surfactants in NB curves [39,40].

TG curve of ODA-B sample showed only one thermal transition with 40% weight loss in the range of 173–650. This weight loss could be assigned to the thermal decomposition of the organo-surfactant.

The ODA-B has the largest weight loss which meant that the amount of the exchanged ODA in the bentonite interlayer was larger than the others modifiers as shown in Table 2. As the molecular weight of the organo-surfactants increased, the exchanged weight content of them increased [36].

It was shown from the thermo-gram of HTAB-B that it had the same weight loss as DDA-B while DDA has lower molecular weight than that of HTAB modifier. This could be explained in terms of main chain carbon number of the surfactants. The exchanged contents in mole of the primary types were higher than those of the tertiary types. In other words, the smaller molecular weight or the smaller molecular diameter was the easier and the deeper diffusion of the organo-surfactant through the interlayer was [41,42]. Also, the silane-B gave the lowest weight loss near to that of the unmodified Na-B because the 3-aminopropyle triethoxysilane was a tertiary type and it had the lowest molecular weight than the others.

From the thermo-grams of NBs it was clear that the thermal stability of these OBs could be arranged in the order Silane-B > DDA-B > HTAB-B > ODA-B. Generally the nano-bentonite was not thermally stable than the ordinary bentonite due to the excess of organic materials. Also the thermal stability decreased as the length of the alkyl group attached to the nitrogen increased [6].

4. Conclusion

Egyptian Bentonite (EB) was modified using four different types of organo-modifiers namely; hexadecyl trimethyl ammonium bromide (HTAB), 3-aminopropyltriethoxysilane (Silane), octadecylamine (ODA) and dodecylamine (DDA). The variation of the EB interlayer space gallery was affected with the type of the used organo-modifiers. The prepared modified EB could be arranged according to its space gallery in the order: (ODA-B > DDA-B > Silane-B > HTAB-B). Generally the nano-bentonite was not thermally stable than the ordinary bentonite due to the excess of organic materials. The thermal stability of the prepared modified bentonites can be arranged in the order: (Silane-B > HTAB-B > DDA-B > ODA-B).

The obtained results indicated that, the ODA modifier can be considered as the more suitable modifier for the modification of the Egyptian Bentonite, whereas it had the highest extent of intercalation. The obtained results promoted the use of the prepared NB as nano-filler for the polymer nanocomposite materials.

References

[1] E. Ruiz-Hitzky, P. Aranda, J.M. Serratosa, in: M. Auerbach, K. Carrado, P.K. Dutta (Eds.), Handbook of Layered Materials, Marcel Dekker Inc., New York, NY, 2004, pp. 91–154 (Chapter 3).

[2] A. Mohanty, in: Proc. Pira Int. Conf., Miami, FL, February 22–24. Nanotechnology for environmentally friendly packaging: current status and future prospects of green/biodegradable nanocomposite materials, 2005.

[3] S.S. Ray, M. Okamoto, Prog. Polym. Sci. 28 (11) (2003) 1539.

[4] M. Kato, A. Usuki, in: T.J. Pinnavaia, G.W. Beall (Eds.), Polymer-Clay Nanocomposites, John Wiley Sons Ltd, New York, 2000, p. 97.

[5] D.H. Solomon, D.G. Hawthorne, Chemistry of Pigments and Fillers, John Wiley & Sons Inc., New York, NY, 1983 (Chapters 1 and 4), pp. 14–16, 21–27, 136–143.

[6] H.K. Neung, V.M. Sanjay, X. Marino, Microporous Mesoporous Mater. 96 (2006) 29–35.

[7] S. Austin, C.H. Patrice, C. Valeska, D.S. Ronald, Polymer 48 (2007) 1490–1499.

[8] G. Baysal, H. Aydin, S. Köytepeb, T. Seckin, Thermochim. Acta 566 (2013) 305–313.

[9] Qilong Tai, Richard K.K. Yuen, Lei Song, Yuan Hua, Chem. Eng. J. 183 (2012) 542–549.

[10] N. Salahuddin, S.A. Abo-El-Enein, A. Selim, O. Salah El-Dien, Appl. Clay Sci. 47 (2010) 242–248.

[11] K.J. Yao, M. Song, D.J. Hourston, D.Z. Luo, Polymer 43 (2002) 1017–1020.

[12] A. Rehab, N. Salahuddin, Mater. Sci. Eng. A 399 (2005) 368–376.

[13] J.K. Mishra, I. Kim, C.-S. Ha, Macromol. Rapid Commun. 25 (2004) 1851–1855.

[14] S.-Y. Moon, J.-K. Kim, C. Nah, Y.-S. Lee, Eur. Polym. J. 40 (2004) 1615–1621.

[15] A.S. Adriana, D. Karim, G.S. Bluma, Appl. Clay Sci. 47 (2010) 414–420.

[16] B.K.G.T. Bergaya, G. Lagaly, Handbook of Clay Science, Developments in Clay Science, Elsevier Ltd., 2006 (Chapter 7.1).

[17] Z. Bouberka, A. Khenifi, F. Sekrane, N. Bettahar, Z. Derriche, Chem. Eng. J. 136 (2007) 295–305.

[18] E. Eren, B. Afsin, Dyes Pigm. 76 (2008) 220–225.

[19] R.R. Adham, M.K.E. Amal, A.G. Ahmed, Appl. Clay Sci. 47 (2010) 196–202.

[20] L. Shichang, Z. Wei, L. Song, S. Wenfang, Eur. Polym. J. 44 (2008) 1613–1619.

[21] A.M. Motawie, M.M. Badr, D.E. Abo-El-Yazid, D.A. El-Komy, Egyptian Patent No. 26250/2013/entitled: Treatment of Egyptian Bentonite to Modified Nano Egyptian Organo-Bentonite.

[22] R.H. Sung, Y.R. Kyong, C.K. Hee, T.K. Jeong, Colloids Surf., A 313–314 (2008) 112–115.

[23] D. García-Lópeza, I. Gobernado-Mitre, J.F. Fernández, J.C. Merino, J.M. Pastor, Polymer 46 (2005) 2758–2765.

[24] Y. Jui-Ming, H. Hsiu-Yin, C. Chi-Lun, S. Wen-Fen, Y. Yuan-Hsiang, Surf. Coat. Technol. 200 (2006) 2753–2763.

[25] R. Zagorka, M. Aleksandra, Eur. Ceram. Soc. J. 27 (2007) 1691–1695.

[26] C. Fenandes, C. Catrinescu, P. Castilho, Appl. Catal., A 318 (2007) 108–120.

[27] D.K. Chattopadhyay, K. Aswini Mishra, B. Sreedhar, K.V.S.N. Raju, Polym. Degrad. Stab. 91 (2006) 1837–1849.
[28] S. Sankaraiah, C. Sung-Wook, L. Jun-Young, K. Jung Hyun, Polymer 48 (2007) 4691–4703.
[29] H.D. Cheol, H.L. Min, D.K. Young, H.M. Byong, H.K. Jeong, Polymer 47 (2006) 6718–6730.
[30] H. Zheng, Y. Zhang, Z. Peng, Y. Zhang, Polym. Test. 23 (2004) 217–223.
[31] D.K. Chattopadhyay, K.V.S.N. Raju, Prog. Polym. Sci. 32 (2007) 352–418.
[32] K. Carrado, L. Xu, R. Csencsits, J. Muntean, Chem. Mater. 13 (2001) 3766–3773.
[33] N.H.M. Zulfli, C.W. Shyang, J. Phys. Sci. 21 (2) (2010) 41–50.
[34] P. Stroeve, Y.C. Ke, Polymer-layered Silicate and Silica Nanocomposites, Elsevier Pub, USA, 2005.
[35] H. Hayden, Developments in Clay Science, 2 Applied Clay Mineralogy Occurrences, Processing and Application of Kaolins, Bentonites, Palygorskite-Sepiolite, and Common Clays, Elsevier Pub., USA, 2005.
[36] J.Y. Lee, H.K. Lee, Mater. Chem. Phys. J. 85 (2004) 410–415.
[37] V.B. Michail, M.S. Kostyantyn, V.S. Valery, P. Policarpos, S. Anna, V.S. Irina, I.T. Vitalij, P.G. Yuri, Polymer 46 (2005) 12226–12232.
[38] K. Thontree, K. Yasushi, U. Toshikazu, N. Diago, T. Wandee, P. Yupin, C. Suwabun, Polymer 49 (2008) 1676–1684.
[39] Y. Qin-Yan, L. Qian, G. Bao-Yu, W. Yan, Sep. Purif. Technol. 54 (2007) 279–290.
[40] F. Huei-Kuan, H. Chih-Feng, H. Jieh-Ming, C. Feng-Chih, Polymer 49 (2008) 1305–1311.
[41] K. Oiuma, K. Kobayashi, in: Proceedings of the 14th National Conference on Clays and Clay Minerals, 1996, pp. 209–219.
[42] S. Karaboni, B. Smith, W. Heidug, J. Vrai, E. Van Ort, Sci. J. 271 (1996) 1102.